Magnetohydrodynamic Models for the Structure of Pulsar-Wind Nebulae

Stephen P. Reynolds

North Carolina State University steve_reynolds@ncsu.edu

1 Abstract

The Crab Nebula is well-described at optical wavelengths and above by a steady-state magnetohydrodynamic model due to Kennel and Coroniti (1984). Can this class of model describe other pulsar-wind nebulae? I exhibit simple generalizations of KC models, for various values of σ, the ratio of magnetic to particle flux input at the wind shock. I calculate the evolution of the electron spectrum and synchrotron emissivity in the nebula assuming spherical symmetry, a steady state, and a purely toroidal magnetic field. Emission profiles depend on the initial magnetic field B_0, the electron spectral index s, and the angle of the toroidal axis with the line of sight, ϕ. I show integrated spectra and radial profiles for various cases, along with predicted variations of photon index Γ with radius in X-rays. Most models predict much smaller sizes in X-rays, and curves of $\Gamma(r)$ which do not resemble observations. Further elaborations of the dynamics of PWNe seem necessary.

2 Introduction

Pulsar-wind nebulae (PWNe) are bubbles of relativistic particles and magnetic field inflated by a pulsar, forming center-brightened radio and X-ray sources of synchrotron radiation [1], [2], [3], [4]. Most early work on PWNe assumed they were surrounded by shell supernova remnants (SNRs), seen or unseen, and interacted with the interior of those remnants. Before the passage of a reverse shock, the PWN would expand into unshocked ejecta in the SNR interior; afterwards, it would be compressed by the reverse-shock passage and expand much more slowly into the thermalized, shocked ejecta [2].

The most elaborate early model for the high-energy (optical and above) emission from PWNe was that of Kennel & Coroniti [3], [4] who solved the steady-state relativistic MHD equations in spherical symmetry with an azimuthal magnetic field to obtain velocity and density profiles of the outflow-

ing relativistic material. They showed that a strong (high compression) MHD shock required a fluid dominated by particles, not magnetic field, as parameterized by $\sigma \equiv (B/4\pi)/n\gamma^2\beta mc^2$, the ratio of magnetic (plus electric) energy flux to particle flux just upstream of the wind shock. Here n is the comoving density and γ the flow Lorentz factor. Applying the Rankine-Hugoniot jump conditions at the wind shock (radius r_s) showed that unless $\sigma \ll 1$, the postshock fluid would remain at high speed, within a factor of 3 of the upstream (relativistic) speed – clearly inconsistent with the observed expansion of the Crab Nebula at $v \sim 2000$ km s^{-1}. Behind the shock, pure flux-freezing meant that the toroidal magnetic field strength evolved as $B \propto \rho r$, with ρ the matter density. Kennel & Coroniti [4] were able then to follow the evolution of electron energies and predict both the integrated spectrum and the brightness profile of remnants. They specialized to the Crab Nebula and showed calculations primarily for that case. They were able to describe the optical through hard X-ray spectrum well, as well as the gross variation of nebular size with X-ray energy ("size" being typically the FWHM of emission measured with relatively crude imaging instruments). However, the high value of preshock Lorentz factor of the wind they found ($\gamma \sim 10^6$) made it difficult to explain the radio emission which requires much lower energies, and more electrons, than would be produced by thermalizing this extremely relativistic wind.

Since the advent of the newer generation of X-ray telescopes, beginning with *ASCA* and continuing with the *Chandra* X-ray Observatory and *XMM-Newton,* we have seen an explosion in the number and variety of PWNe in X-rays, and have observed a much wider range of morphological type. It is of interest to ask if the class of steady-state MHD models proposed by KC can be generalized appropriately to describe other PWNe, and if not, to get an idea of what kind of extensions might be necessary. This is the project described in this paper.

One major problem in modeling several larger, fainter PWNe such as 3C 58 [5] appears in comparing radio and X-ray images. In Kennel & Coroniti's model for the Crab, synchrotron losses on outflowing particles cause the nebular size to decrease with frequency at optical and higher frequencies. In fact the Crab is considerably smaller at optical than radio frequencies, and continues to diminish in size roughly as $R \propto \nu^{-0.15}$ up to 40 keV [6]. However, 3C 58 shows X-ray emission extending to near the edges of the radio emission, though it is faint there (Slane, private communication). These results call into question the MHD picture of transport of particle energy and magnetic flux throughout the volume of a PWN.

It is straightforward to show from the MHD equations [3] that postshock flow solutions have accelerating and decelerating branches, with the latter beginning at $v_0 = c/3$ and initially decelerating as r^{-2} (pure hydrodynamic, isobaric flow; magnetic energy is unimportant since σ must be small to fit the outer nebular boundary conditions). However, in this case $B \propto \rho r \propto 1/rv \propto r$, so the magnetic energy *rises* until it becomes dynamically important, slowing the deceleration and causing the velocity to approach a constant value, with

$B \to 1/r$. The full hydrodynamic solution can be well approximated by a simple analytic form: defining $u \equiv v/v_0$,

$$u(r) = \frac{1}{r^2}(1 - u_\infty) + u_\infty, \tag{1}$$

where the asymptotic velocity is $v_\infty/c = \sigma/(1+\sigma)$ (Fig. 1).

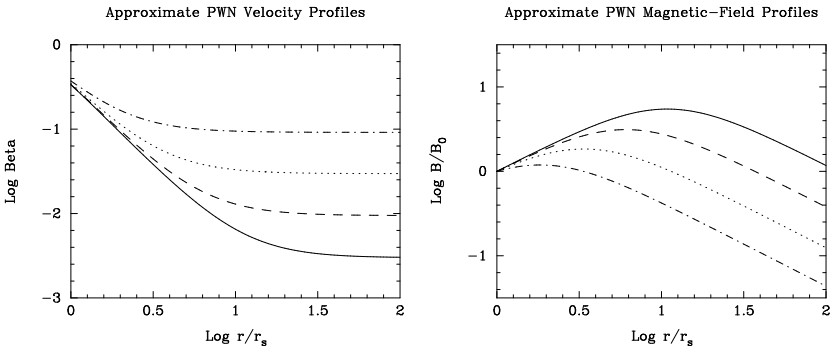

Fig. 1. Solid lines: $\sigma = 0.001$. Dashed lines: $\sigma = 0.0032$. Dotted lines: $\sigma = 0.01$. Dot-dashed lines: $\sigma = 0.032$.

3 Particle evolution and luminosity calculation

Electron energies E evolve due both to radiative and adiabatic losses: $\dot{E} = (dE/dV)(dV/dt) - aB^2E^2$, where for synchrotron losses $a = 1.57 \times 10^{-3}$ cgs. This equation can be integrated to give [4], [7]

$$E(t) = \frac{E_0\alpha^{1/3}}{1 + aE_0 \int B^2\alpha^{1/3}dt} = \frac{E_0\alpha^{1/3}}{1 + E_0\left(\frac{aB_0^2r_0}{v_0}\right)\int z^{-8/3}u^{-10/3}dz} \tag{2}$$

where $\alpha \equiv \rho/\rho_0$, $z \equiv r/r_0$, and $u \equiv v/v_0$. The quantity $E_f \equiv (aB_0^2r_0/v_0)^{-1}$ is a "fiducial energy", that an initially infinitely energetic electron would have after radiating in a field B_0 for a time r_0/v_0 (basically a parameterization of B_0). From this result, the evolution of an arbitrary distribution can be calculated:

$$N(E) = N(E_0)\frac{dE_0}{dE}\frac{dV_0}{dV} = N(E_0(E))\frac{dE_0}{dE}\alpha = N(E_0(E))\left(\frac{E_0^2}{E^2}\right)\left(\frac{\rho}{\rho_0}\right)^{4/3}. \tag{3}$$

Given the approximate dynamics above, the electron distribution and synchrotron emissivity can be calculated numerically at each radius. If magnetic

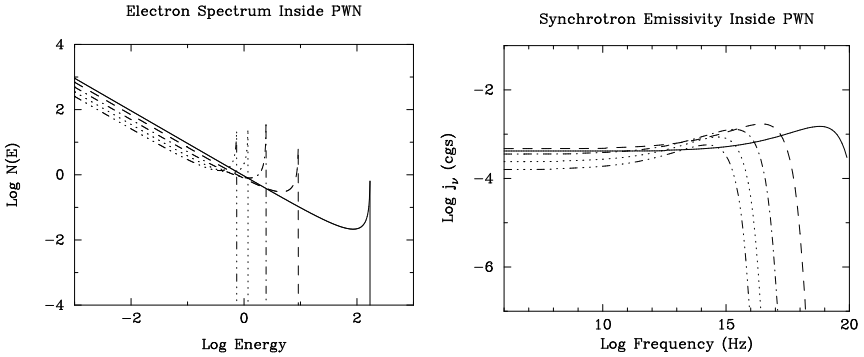

Fig. 2. Flat-spectrum, high-σ case: $s = 1.0$, $\sigma = 0.01$, $E_f = 910$ erg, and $E_{\rm min} = 10^{-5}$ erg. From left to right, lines show the spectrum and emissivity at five radii (outside in): $r/r_0 = 10, 8, 6, 4, 2$.

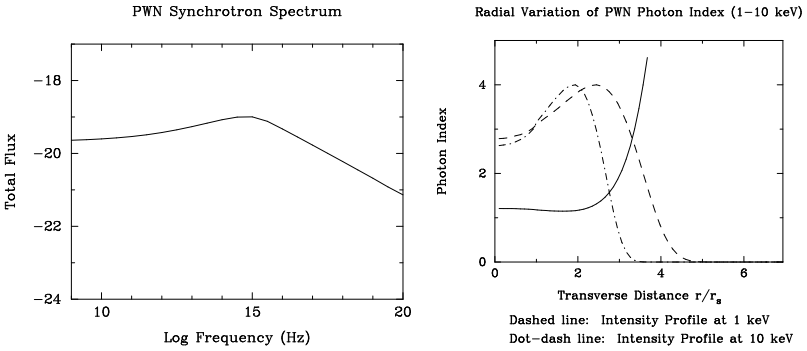

Fig. 3. Same parameters as above. Note curvature of the integrated spectrum due to the energy-loss "bump". The solid line on the right is the 1–10 keV photon index; the profiles are for aspect angle $\phi = 0^\circ$ (**B** in the plane of the sky).

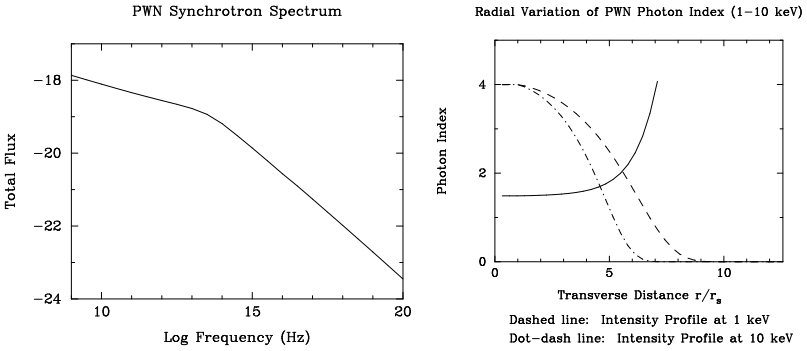

Fig. 4. Steeper-spectrum, low-σ case: $s = 1.5$, $\sigma = 0.001$, $E_f = 9.1 \times 10^5$ erg, and aspect angle $\phi = 90^\circ$.

field lines are circles in an equatorial plane, an elementary rotation can give brightness profiles as a function of aspect angle ϕ between the polar axis and the line of sight. The synchrotron emissivity was integrated numerically to generate the brightness profiles shown above, for an injected flat power-law $N(E) = KE^{-s}$ with $s < 2$ as deduced from observed PWN radio spectra. The flat spectra cause a "bump" to appear just below the high-energy cutoff that appears as a result of radiative losses.

4 Conclusions

Steady-state MHD models of pulsar-wind nebulae can be well approximated by a simple velocity law, which then dictates the evolution of the injected electron distribution and the integrated spectrum and profile of emission, depending on σ. Spectral properties also depend on $\mathbf{B}$ and spectral index s. Varying the aspect angle changes the flux normalization but has no effect on the integrated spectrum and little on the profile shape at photon energies for which losses are important. For very flat injected spectra ($s \sim 1$), the effects of the energy-loss "bump" are significant, causing concave-up curvature over a broad frequency range.

The models are in significant conflict with the observed radial dependence of photon index Γ in X-rays (e.g., G21.5-0.9 [8]), which appears roughly linear with r. All models drop in size by at least a factor 2 between radio and X-rays, but some observed PWNe do not show this. Unless magnetic-field strengths are unrealistically low, most X-ray profiles have HWHM radii only 3–6 times the injection radius – also perhaps at odds with observations.

We conclude that there are significant discrepancies between the predictions of the simple MHD models and X-ray observations of PWNe. Nonsteady or nonspherical flows, and/or electron transport by diffusion as well as convection (e.g., [9]), may be necessary to explain the observations.

References

1. K.W. Weiler, N. Panagia: Astron. Astrophys. **90**, 269 (1980)
2. S.P. Reynolds, R.A. Chevalier: Astrophys.J. **278**, 630 (1984; RC84)
3. C.F. Kennel, F.V. Coroniti: Astrophys.J. **283**, 694, (1984)
4. C.F. Kennel, F.V. Coroniti: Astrophys.J. **283**, 710 (1984)
5. K. Torii, P.O. Slane, K. Kinugasa et al: Pub. Astron. Soc. Japan **52**, 875 (2000)
6. W. Ku, H.L. Kestenbaum, R. Novick et al: Astrophys.J. **204**, L77 (1976)
7. S.P. Reynolds: Astrophys.J. **493**, 375 (1998)
8. P.O. Slane, Y. Chen, N.S. Schulz et al: Astrophys.J. **533**, L29 (2000)
9. S.P. Reynolds, F.C. Jones: *Proc. 22nd ICRC (Dublin)*, **2**, 400 (1991)